

Rational Screening Approach for Classical Chiral Resolution under Thermodynamic Equilibrium: A Case Study of Diphenyl-Substituted *N*-Methyl-Piperazine

Helming Tan,^{*,†} Sheng Cui,^{*,†} Kyung Gahm,[‡] Van Luu,[†] and Shawn D. Walker[†]

Small Molecule Process and Product Development, and Discovery Analytical Science, Chemistry Research & Discovery, Amgen Inc., One Amgen Center Drive, Thousand Oaks, California 91320, United States

Abstract:

Separation of racemic mixtures by the formation and crystallization of diastereomeric salts (classical resolution) is an important process in the pharmaceutical industry. We have developed and implemented a high-throughput screening workflow to effectively guide the development and optimization of a thermodynamically favored resolution process. A case study is presented for optical resolution of a diphenyl-substituted *N*-methyl-piperazine derivative, a racemic compound with a eutectic point of 60% *ee*. Through a rational screening approach, the effect of equilibrium solubility on resolution efficiency was systematically evaluated with regards to resolving agent, solvent composition, resolving agent stoichiometry, and racemate concentration. An isothermal solubility phase diagram was obtained, and solid-state characterization was performed on the diastereomeric salts to understand their phase behaviors under the optimal resolution conditions. The highest resolution efficiency was achieved when the diastereomeric hemi-salt tetrahydrate was formed with 0.35 mol equiv of di-*p*-anisoyl-*D*-tartaric acid in THF/H₂O (80/20, v/v), while a solid solution of desired and undesired diastereomeric salts crystallized with 70% *de*. After salt break, the desired enantiomer was upgraded to 98% *ee* by recrystallization twice in *n*-heptane. These screening results led to a successful resolution of 30 g racemate with a yield of 37%. This case study demonstrated that the rational screening approach is effective in guiding scale-up for classical chiral resolution under thermodynamic equilibrium.

1. Introduction

Introduced by Louis Pasteur in 1853,¹ classical resolution is often considered as one of the most efficient methods to produce enantiopure pharmaceuticals on a large scale.^{2,3} In the classical resolution, a racemic acid or base reacts with a chiral resolving agent to form two diastereomeric salts, which exhibit different physicochemical properties, notably solubility,⁴ and can therefore be separated by fractional crystallization. Though the crystallization can be kinetically controlled, the diastereomeric salts are preferably separated under equilibrium conditions so that an optimal resolution process can be drawn on the

solubility phase diagrams.⁵ However, the theoretical background of the classical resolution is, in general, poorly understood, and the resolution system is often selected on the basis of experimental trial-and-error.⁶ A systematic experimentation approach has been introduced to investigate the governing parameters for preferential diastereomeric salt crystallization, which are resolving agent, solvent, molar ratio of resolving agent to racemate, and racemate concentration.⁷ The main limitation has been the time taken in screening for the optimal resolving agent and the solvent system in order to achieve the highest resolution efficiency. Commonly a collection of low-cost resolving acids or bases is screened.⁸ In the so-called “Dutch resolution”, several members of structurally related resolving agents are used together to facilitate the precipitation of the least soluble diastereomeric salt mixture.⁹ In addition to the resolving agent, the solvent system (including the mixture with water) can greatly affect the resolution efficiency by altering composition and solubility through formation of crystalline solvates or hydrates.¹⁰

A number of methods to guide resolving agent selection have been reported. To effectively identify chiral resolving agents forming diastereomeric salts with the racemates to be solved, differential scanning calorimetry (DSC) technique has been used in screening the resolving agents by obtaining a distinctive eutectic point of the diastereomeric salts in a binary melting phase diagram.¹¹ To establish an efficient resolution process on the basis of thermodynamic equilibrium, HPLC screening methodology has been reported for determination of the eutectic composition of the mother liquor during diastereomeric salt crystallization.¹² By means of automation and miniaturization in recent years, high-throughput experimentation has emerged as a new approach for screening the optimal crystallization conditions while saving time and material. Recent examples

* To whom correspondence should be addressed. Email: helmingt@amgen.com; scui@amgen.com.

[†] Small Molecule Process and Product Development.

[‡] Discovery Analytical Science, Chemistry Research and Discovery.

- (1) Pasteur, L. *C. R. Hebd. Seances Acad. Sci.* **1853**, 37, 162.
- (2) Collet, A. *Angew. Chem., Int. Ed.* **1998**, 37, 3239.
- (3) Fogassy, E.; Nógrádi, M.; Pálovics, E.; Schindler, J. *Synthesis* **2005**, 10, 1555.
- (4) Armstrong, M. D. *J. Am. Chem. Soc.* **1951**, 73, 4456.

- (5) Marchand, P.; Lefebvre, L.; Querniard, F.; Cardinael, P.; Perez, G.; Counioux, J.; Coquerel, G. *Tetrahedron: Asymmetry* **2004**, 15, 2455.
- (6) Ferreira, F. C.; Ghazali, N. F.; Cocchini, U.; Livingston, A. G. *Tetrahedron: Asymmetry* **2006**, 17, 1337.
- (7) Jacques, J.; Collet, A.; Wilen, S. H. *Enantiomers, Racemates and Resolutions*; Krieger Publishing Co.: Florida, 1994.
- (8) Kozma, D. *CRC Handbook of Optical Resolutions via Diastereomeric Salt Formation*, CRC Press: Boca Raton, FL, 2002.
- (9) Vries, T.; Wynberg, H.; van Echten, E.; Koek, J.; ten Hoeve, W.; Kellogg, R. M.; Broxterman, Q. B.; Minnaard, A.; Kaptein, B.; van der Sluis, S.; Hulshof, L.; Kooistra, J. *Angew. Chem., Int. Ed.* **1998**, 37, 2349.
- (10) Sakai, K.; Sakurai, R.; Yuzawa, A.; Kobayashi, Y.; Saigo, K. *Tetrahedron: Asymmetry* **2003**, 14, 1631.
- (11) Dyer, U. C.; Henderson, D. A.; Mitchell, M. B. *Org. Process Res. Dev.* **1999**, 3, 161.
- (12) Borghese, A.; Libert, V.; Zhang, T.; Alt, C. A. *Org. Process Res. Dev.* **2004**, 8, 532.

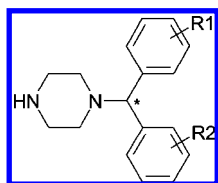


Figure 1. Structure of diphenyl-substituted *N*-methyl-piperazine.

include salt and polymorph screening,¹³ and purification screening of impure compounds by crystallization on 96-well plates.¹⁴ However, there has been no report in high-throughput screening methodology to identify the optimal resolution system by systematically evaluating the key resolution parameters including resolving agent, solvent composition, molar ratio of resolving agent to racemate, and racemate concentration. In this report we have developed and implemented a high-throughput chiral resolution screening workflow in a 96-well plate format, and we present a case study of classical chiral resolution via differential diastereomeric salt crystallization under thermodynamic equilibrium.

R_1, R_2 -Substituted diphenyl-*N*-methyl piperazine (Figure 1) is an important structural motif present in many pharmaceutical lead candidates. One of the derivatives we are interested in has a chiral center and exists as a racemic compound. In our rational screening approach to resolve this racemic compound, eight chiral resolving acids were selected, and each acid was screened in 12 solvents (including their mixtures with water). A chiral HPLC method was used to determine the thermodynamic solubility of the diastereomeric salts formed under defined screening conditions. On the basis of mass balance in each salt crystallization system, the maximum yield, diastereomeric excess (*de*), and resolution efficiency of desired diastereomeric salt (DDS) were calculated and evaluated for the selection of the optimal resolution system. The effect of solvent, particularly water, on the resolution efficiency was investigated. The racemate concentration and the molar equivalent of the resolving agent were investigated to further optimize the resolution conditions. The chemical composition and the solid-state properties of the crystallized diastereomeric salt were also characterized. Finally, a solubility phase diagram was constructed based on the optimal resolution system resulting from our high throughput screening approach, which led to a successful resolution of the racemic diphenyl-substituted *N*-methyl-piperazine compound at a scale of 30 g.

1.1. Physicochemical Characterization of a Racemic Compound. The diphenyl-substituted *N*-methyl-piperazine (referred to as the piperazine hereafter) racemate as well as its enantiopure desired and undesired isomers were internally obtained. In order to define the type of racemate (conglomerate, racemic compound, or solid solution),¹⁵ X-ray powder diffraction (XRPD), differential scanning calorimetry (DSC), and

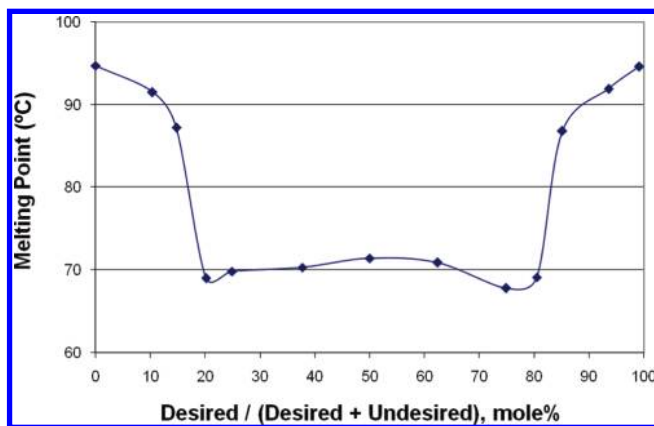


Figure 2. Melting-phase diagram of the racemic piperazine mixture.

thermogravimetric analysis (TGA) were performed. The XRPD patterns between the racemate and the enantiomers were distinctively different, whereas by DSC the melting point of the racemate (65 °C) was lower than that of the enantiomer (95 °C). TGA showed no weight loss upon heating to melting, thus the solid forms were anhydrous. These data indicated that the racemate could be either a racemic compound or a conglomerate of a metastable polymorph of the enantiomer. To test these two possibilities, slurry experiments were performed at room temperature by mixing the racemate and the enantiomer (50/50, w/w) in water/tetrahydrofuran (THF) and *n*-heptane/methyl *tert*-butyl-ether (MTBE), respectively. The slurry samples were filtered after 24 h and the solid was analyzed by XRPD for possible form conversion. The XRPD patterns displayed the unchanged form mixtures of the racemate and the enantiomer, suggesting that the racemate is likely a racemic compound. To further confirm a racemic compound and to determine its eutectic point through construction of a melting phase diagram, solid samples with various enantiomeric excess (*ee*) were prepared by dissolving different amounts of enantiopure desired and undesired isomers in MTBE followed by evaporation, and the recovered solids were analyzed by DSC. A nearly symmetric melting point curve was obtained (Figure 2), showing a eutectic point close to 60% *ee*, with a variation of 4 °C in melting of racemic mixtures over a range of 20 – 80 mol %. The melting results proved the piperazine to be a racemic compound that could be enantiomerically purified via crystallization in an appropriate solvent when its racemic mixture was great than 60% *ee*. This finding prompted us to develop a two-step resolution strategy suitable for this racemic compound: 1) formation of diastereomeric salts with a minimum *de* of 60% in an optimal resolution system; 2) break of diastereomeric salt and upgrade of the desired enantiomer to $\geq 98\%$ *ee* by crystallization of the piperazine freebase in a proper solvent.

1.2. Selection of Chiral Resolving Agents. Eight commercially available acids were selected as shown in Table 1. In the initial screen to explore the diastereomeric salt selectivity, the naturally abundant L-enantiomer was added at a half molar ratio to the racemate. The hits from the resolving agents were those whose diastereomeric salt pair exhibited different solubility. Subsequently in the follow-up screen, either L- or D-enantiomers was selected to form DDS with a lower solubility,

- (13) Carlson, E. D.; Cong, P.; Chandler, W. H., Jr.; Chau, H.; Crevier, T.; Desrosiers, P. J.; Doolen, R. D.; Freitag, C.; Hall, L. A.; Kudla, T.; Luo, R.; Masui, C.; Rogers, J.; Song, L.; Tangkilisan, A.; Ung, K. Q.; Wu, L. *PharmaChem* **2003**, 10.
- (14) Tan, H.; Reed, M.; Gahm, K. H.; King, T.; Seran, M. D.; Bostick, T.; Luu, V.; Semin, D.; Cheetham, J.; Larsen, R.; Martinelli, M.; Reider, P. *Org. Process Res. Dev.* **2008**, 12, 58.
- (15) (a) Coquerel, G. *Enantiomers* **2000**, 5, 481. (b) Collet, A. *Enantiomers* **1999**, 4, 157.

Table 1. Resolution efficiency of diastereomeric salts in the initial screen (racemate 40 mg/mL, 0.5 mol equiv of resolving agent to racemate; the blank cells indicate a clear solution and no salt formation)

| resolving agent (source) | acetone/H ₂ O | | THF/H ₂ O | | MeCN/H ₂ O | | MeOH/H ₂ O | | EtOH/H ₂ O | | IPA | IPA/H ₂ O |
|--|--------------------------|-------------|----------------------|---------|-----------------------|---------|-----------------------|---------|-----------------------|---------|------|----------------------|
| | acetone | (80/20) | THF | (80/20) | MeCN | (80/20) | MeOH | (80/20) | EtOH | (80/20) | | |
| L-malic acid (Fluka) | | | | | | | | | | | | |
| L-tartaric acid (Aldrich) | | | | | | | | | | | | |
| (+)-camphoric acid (Aldrich) | 0.04 | | | | 0.01 | | | | | | 0.01 | |
| dibenzoyl-L-tartaric acid (Fluka) | 0.01 | 0.01 | 0.01 | | 0.01 | -0.22 | -0.02 | -0.02 | -0.02 | -0.33 | 0.01 | -0.31 |
| di- <i>p</i> -toluoyl-L-tartaric acid (Fluka) | | 0.21 | | | | 0.09 | -0.02 | -0.03 | | | 0.01 | 0.02 |
| di- <i>p</i> -anisoyl-L-tartaric acid (TCI) | -0.01 | -0.05 | -0.14 | -0.62 | 0.04 | -0.13 | 0.46 | -0.02 | 0.06 | -0.03 | 0.01 | -0.02 |
| di- <i>p</i> -pivaloyl-L-tartaric acid (Fluka) | 0.01 | | | | 0.01 | | | | | | | |
| <i>N</i> -Cbz-L-aspartic acid (Aldrich) | 0.01 | | | | -0.01 | | | | | | | |

Table 2. Resolution efficiency of diastereomeric salts in the follow-up screen (racemate 40 mg/mL, 0.5 mol equiv of resolving agent to racemate; the blank cells indicate a clear solution and no salt formation)

| resolving efficiency (S) | binary solvent | 0% | 5% | 10% | 15% | 20% | 25% | 30% | 35% | 40% | 45% | 50% |
|--|----------------|------------------|------------------|------------------|------------------|------------------|------------------|------------------|------------------|------------------|------------------|------------------|
| | | H ₂ O | H ₂ O | H ₂ O | H ₂ O | H ₂ O | H ₂ O | H ₂ O | H ₂ O | H ₂ O | H ₂ O | H ₂ O |
| dibenzoyl-D-tartaric acid (D-DBTA) (Fluka) | MeCN | 0.01 | 0.01 | 0.03 | 0.11 | 0.23 | 0.30 | 0.37 | 0.27 | 0.20 | 0.17 | 0.15 |
| dibenzoyl-L-tartaric acid (L-DBTA) (Fluka) | EtOH | 0.01 | 0.01 | 0.01 | 0.30 | 0.37 | 0.37 | 0.37 | 0.25 | 0.11 | 0.07 | 0.06 |
| dibenzoyl-D-tartaric acid (D-DBTA) (Fluka) | IPA | 0.01 | 0.01 | 0.07 | 0.34 | 0.36 | 0.31 | 0.35 | 0.23 | 0.21 | 0.09 | 0.07 |
| di- <i>p</i> -toluoyl-L-tartaric acid (L-DTTA) (Fluka) | acetone | | | | | 0.30 | 0.27 | 0.30 | 0.36 | 0.39 | 0.25 | 0.17 |
| di- <i>p</i> -anisoyl-D-tartaric acid (D-DATA) (AK Scientific) | THF | 0.17 | 0.56 | 0.59 | 0.61 | 0.62 | 0.60 | 0.62 | 0.60 | 0.59 | 0.19 | 0.14 |
| di- <i>p</i> -anisoyl-D-tartaric acid (D-DATA) (AK Scientific) | MeCN | 0.01 | 0.01 | 0.03 | 0.07 | 0.11 | 0.13 | 0.11 | 0.11 | 0.10 | 0.10 | 0.06 |
| di- <i>p</i> -anisoyl-L-tartaric acid (L-DATA) (AK Scientific) | MeOH | 0.49 | -0.20 | -0.02 | -0.01 | -0.03 | -0.03 | -0.04 | -0.06 | -0.02 | -0.03 | -0.01 |

while the molar equivalent of resolving agent was varied to achieve the optimal *de* and yield.

1.3. Selection of Solvents. Six pure solvents, acetone, THF, acetonitrile (MeCN), methanol (MeOH), ethanol (EtOH), and isopropanol (IPA), as well as six solvent mixtures of each with 20% water, were selected in the initial screen (Table 1). If a water mixture solvent was a hit from the initial screen, water mixture solvents from 95/5 to 50/50 (v/v) with an increment of 5% water were selected in the follow-up screen (Table 2) to evaluate the solubility/hydration effect of water.

1.4. Birefringence Microscopic Imaging. The initial and the follow-up screen experiments were conducted in 1 mL glass

vials on a 96-well plate. A birefringence microscopic image of the 96-well plate was acquired to indicate whether diastereomeric salt was crystallized in each vial under different screening conditions. Figure 3 showed a 96-well image from the initial screening with a racemate loading concentration of ca. 40 mg/mL. The white birefringence images of the wells indicated that individual diastereomeric salts crystallized and the solubility of one corresponding enantiomer was less than 20 mg/mL, whereas the black birefringence images of the wells indicated that clear solutions were present in the vials thus no diastereomeric salt crystallized under the screening conditions. To determine the mother liquor *de* and the solubility of the

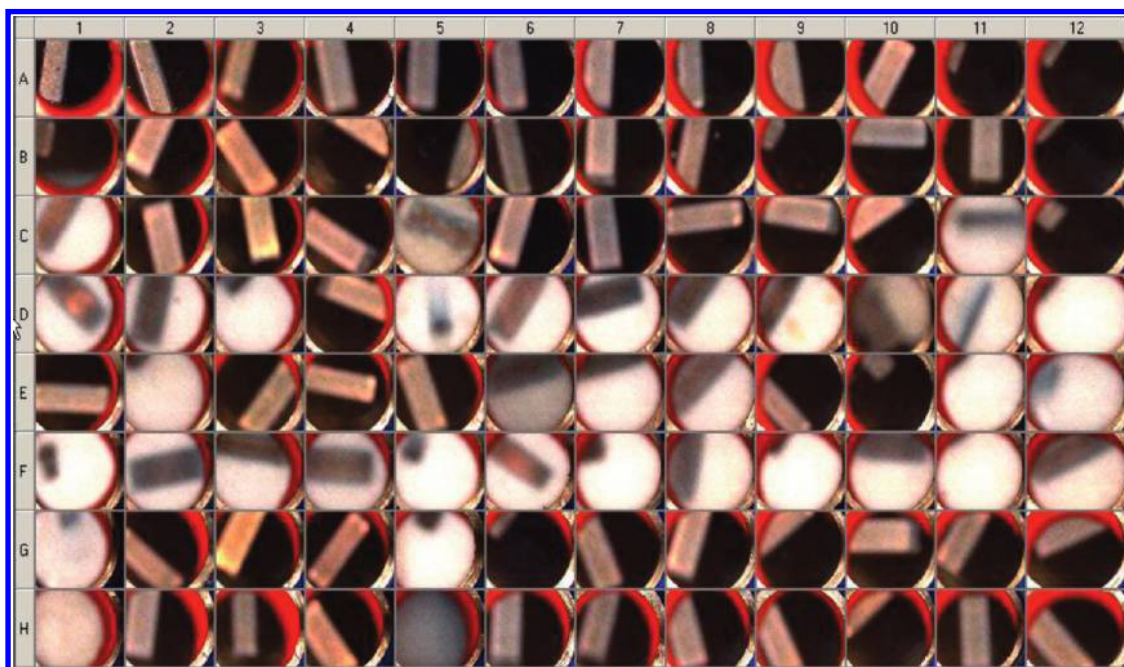


Figure 3. Microscopic birefringence images of a 96-well plate in the initial screen (the same conditions in Table 1).

crystallized diastereomeric salts, supernatant samples were taken and diluted for chiral HPLC analysis.

1.5. Chiral HPLC for Diastereomeric Excess (de) and Solubility Measurement. A normal phase chiral LC/UV method was developed to separate the racemic mixture. A typical chromatogram is shown in Figure 4A. The solubility of DDS and undesired diastereomeric salt (UDS) crystallized under the screening conditions was determined by HPLC quantification on the concentration of the desired and undesired enantiomers in solution. The mother liquor *de* was obtained from the difference in peak area percent between the desired and undesired enantiomers. The chromatograms of representative initial and follow-up screening samples are shown in Figure 4B and 4C.

1.6. Evaluation of Screening Results. The screening results were evaluated with regards to maximum yield, crystal *de*, and resolution efficiency based on mass balance calculation for a mixture of racemate and resolving agent in a closed solvent system. The results were exemplified with the representative initial and follow-up screening samples shown in Figure 4B and 4C. The purpose of a chiral resolution screen is to identify a resolution system with the highest resolution efficiency (*S*).

$$\text{Solubility Ratio } \alpha = \frac{1 + de_{ml}}{1 - de_{ml}} \quad (\text{ml} = \text{mother liquor})$$

$$\text{Maximum Yield } y = 0.5 \times \left(1 - \frac{1}{\alpha}\right)$$

(Theoretical maximum yield 50%)

$$de_{\text{crystal}} = \frac{\text{Solubility}_{\text{undesired}} - \text{Solubility}_{\text{desired}}}{\text{Concentration}_{\text{racemate}} - \text{Solubility}_{\text{undesired}} - \text{Solubility}_{\text{desired}}}$$

$$\text{Resolution Efficiency } (S) = 2 \times y \times de_{\text{crystal}}$$

(*S* = 1 for complete resolution)

2. Results and Discussion

2.1. Initial Screening for Resolving Agent and Solvent Hits. As indicated by the white birefringence images shown in Figure 3, crystalline diastereomeric salts formed in 36 different resolution systems out of the use of 8 resolving acids and 12 solvents in the initial screen when a solution of 40 mg/mL of the piperazine racemate was mixed with 0.5 molar equivalent of the resolving acid. Correspondingly, resolution efficiency was calculated in Table 1 for each of these 36 resolution systems. For example, the salts formed with (+)-camphoric acid in acetone (C1), MeCN (C5), and IPA (C11), with *N*-cbz-L-aspartic acid and di-*p*-pivaloyl-L-tartaric acid in acetone (G1, H1) and MeCN (G5, H5), respectively; however, their solubility difference between DDS and UDS was so small that the resulting resolution efficiency was lower than 0.05 in Table 1. On the other hand, the black birefringence images in Figure 3 indicated no diastereomeric salts crystallized under the screening conditions; therefore the mother liquor was not sampled for chiral LC analysis and the resolution efficiency is not shown in Table 1.

The benzoyl derivatives of tartaric acid generated a number of salt hits with different resolution efficiencies (Table 1).

Notably, diastereomeric salts of di-*p*-anisoyl-L-tartaric acid (L-DATA) crystallized in all twelve solvents screened. The highest resolution efficiency (*S* = −0.62) was achieved with L-DATA in THF/H₂O (80/20), indicating that di-*p*-anisoyl-D-tartaric acid (D-DATA) should be used for preferential crystallization of DDS. It was also noted that the solvent, particularly water, had significant effects on diastereomeric salt selectivity and resolution efficiency. With L-DATA, UDS preferentially crystallized in THF (*S* = −0.14), and its resolution efficiency increased to −0.62 in THF/H₂O (80/20). With the same resolving acid, however, DDS preferentially crystallized in MeOH (*S* = 0.46), and its resolution efficiency dramatically decreased to −0.02 in MeOH/H₂O (80/20).

On the basis of the resolution efficiency results in Table 1, seven resolution systems (including resolving acid and water/solvent mixtures) with *S* ≥ 0.1 were selected for a follow-up screen. These are: D-DATA in THF/H₂O and MeCN/H₂O, L-DATA in MeOH/H₂O, dibenzoyl-D-tartaric acid (D-DBTA) in MeCN/H₂O, EtOH/H₂O, and IPA/H₂O, and di-*p*-toluoyl-L-tartaric acid (L-DTTA) in acetone/H₂O. The purpose of the follow-up screen was to identify and confirm the optimal resolving agent and solvent system from the initial screen hits.

2.2. Follow-up Screening for the Optimal Resolving Agent and Solvent System. Four hit resolving acids, D-DATA, L-DATA, D-DBTA, and L-DTTA were screened at a half molar ratio to the racemate at a concentration of 40 mg/mL in selected solvents as shown in Table 2. To further investigate the effect of water on the resolution efficiency, the water percent increased from 5% to 50% in 5% increments for all of the water mixture solvents. It was found that the presence of water could increase or decrease the solubility of DDS and/or UDS, thus altering the resolution efficiency arising from the difference in solubility between DDS and UDS. In the case of L-DATA in MeOH/H₂O (Figure 5 and Table 2), the solubility of UDS was much higher than that of DDS in MeOH, and a resolution efficiency of 0.49 was obtained; however with the presence of 5–50% water in MeOH, resolution with L-DATA was unfavorable as the solubility of UDS decreased dramatically and became even lower than that of DDS. On the other hand, in the case of D-DATA in THF/H₂O (Figure 6 and Table 2), the solubility of DDS decreased dramatically from 15 mg/mL in THF to less than 3 mg/mL in the mixtures of THF with 5% water or greater, while the solubility of UDS kept around 16–17 mg/mL and insignificantly affected by water up to 40% in THF. Hence, higher yield and higher *de* of DDS were maintained with D-DATA in the mixture of THF and water. The water effect on improving the resolution efficiency was also observed in other resolution systems, i.e., D-DATA in MeCN/H₂O, D-DBTA in MeCN/H₂O, EtOH/H₂O, and IPA/H₂O, and L-DTTA in acetone/H₂O; however, their resulting resolution efficiencies were lower than that of D-DATA in THF/H₂O.

From the follow-up screening results in Table 2, higher resolution efficiency (*S* = 0.56–0.62) was achieved with D-DATA and 5–40% water in THF. However, the optimal water percent deemed to be further explored and derived from the highest resolution efficiency as related to stoichiometry of D-DATA in formation and crystallization of DDS.

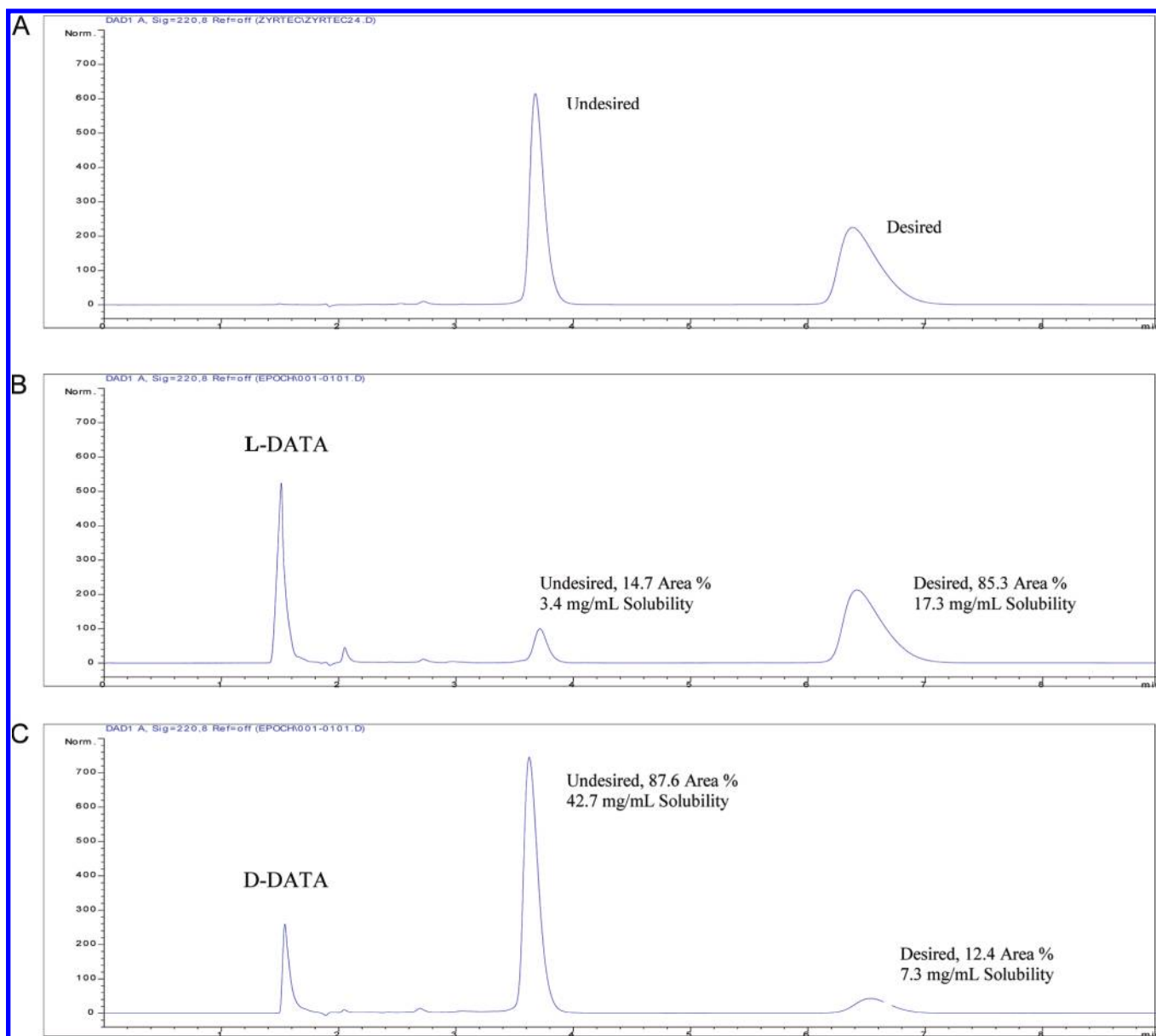


Figure 4. (A) Chiral LC chromatogram of the racemate solution (4.0 mg/mL in MeOH, 220 nm). (B) Chiral LC chromatogram of an initial screening sample (39.0 mg/mL of racemate with 0.50 mol equiv of L-DATA in THF/H₂O, 80/20). DDS crystal *de* –76%, maximum yield 41%, and resolution efficiency –0.62 based on mass balance calculation. (C) Chiral LC chromatogram of a follow-up screening sample (98.7 mg/mL of racemate with 0.35 mol equiv of D-DATA in THF/H₂O, 80/20). DDS crystal *de* 73%, maximum yield 42%, and resolution efficiency 0.61 based on mass balance calculation.

2.3. Screening for the Optimal Resolving Agent Stoichiometry and Water Mixture Solvent. D-DATA was identified and confirmed to be the optimal resolving agent, and the effect of the resolving agent stoichiometry on the resolution efficiency was then evaluated in THF/H₂O mixtures. As shown in Figure 7 at a racemate concentration of 100 mg/mL, the resolution efficiency was consistently high when the molar ratio of D-DATA to the racemate was in a range of 0.3 – 0.4 with 15 – 30% water in THF. Given the highest efficiency of 0.61, the optimal stoichiometry and solvent were consequently determined to be 0.35 mol equiv of D-DATA in THF/H₂O (80/20). The stoichiometry of the resolving acid suggested that DDS could be a hemitartrate, with the equilibrium schemes shown in Figure 8. Although crystallization of DDS was thermodynamically favored over UDS as driven by their difference in solubility, the relatively lower resolution efficiency at 0.25 mol

equiv of the resolving acid suggested that UDS could be cocrystallized with DDS to form a solid solution and solid-state characterization of the isolated salt deemed necessary. When 0.50 equiv of the resolving acid was used, the resolution efficiency decreased as the crystallization yield of UDS increased. The resolution efficiency further decreased when 0.75 or 1.0 equiv of the resolving acid was used, presumably due to the common ion effect largely on the solubility of UDS. At the optimal (0.35) molar equivalent of D-DATA, DDS preferentially crystallized at maximum yield. It is postulated in Figure 8 that DDS was in equilibrium with the free desired enantiomer in the solution phase and also with UDS partially crystallized in the solid phase, which, in turn, was in equilibrium with the free undesired enantiomer in the solution phase.

2.4. Effect of Racemate Concentration. As part of resolution process development, the effect of the racemate concentra-

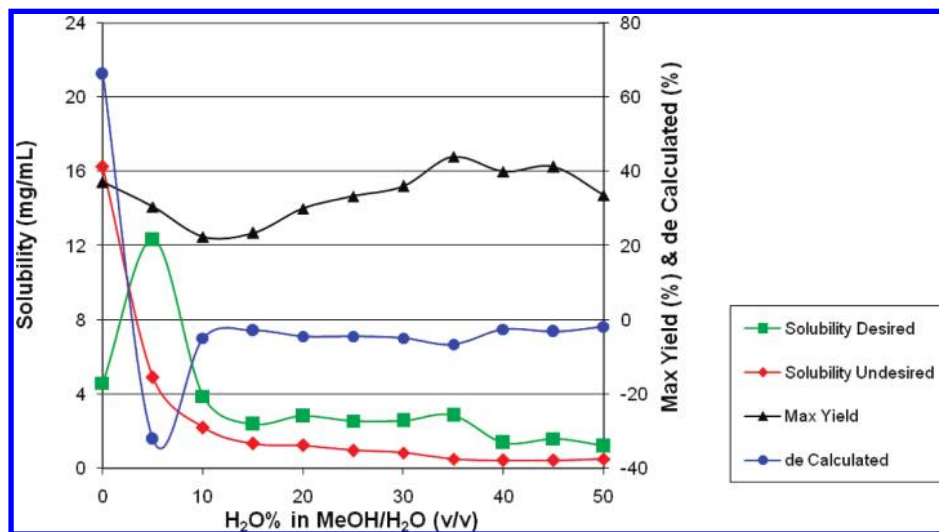


Figure 5. Solubility, maximum yield, and calculated *de* of DDS with 0.5 mol equiv of L-DATA in MeOH/H₂O at a racemate concentration of 40 mg/mL.

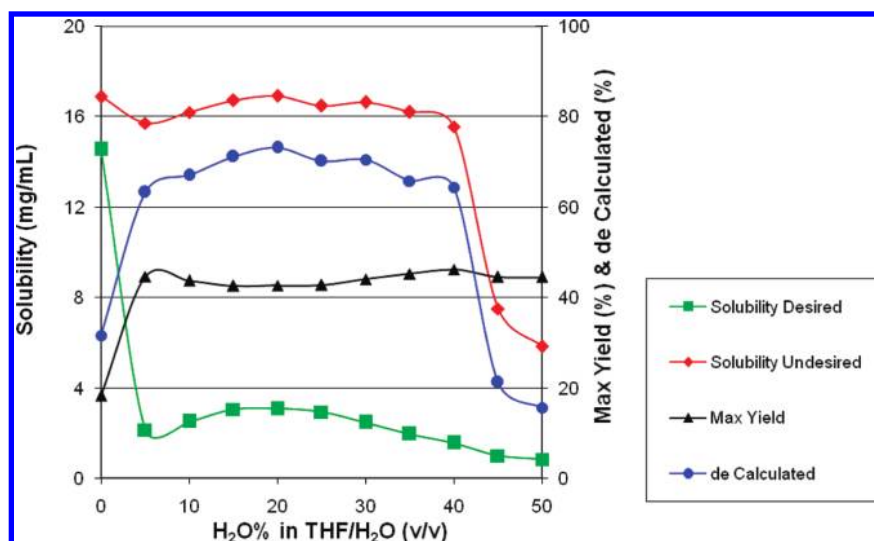


Figure 6. Solubility, maximum yield, and calculated *de* of DDS with 0.5 mol equiv of D-DATA in THF/H₂O at a racemate concentration of 40 mg/mL.

tion on the resolution efficiency was investigated with the optimal resolution system identified. As shown in Figure 9A, the apparent solubility of both DDS and UDS, or the concentration of the free enantiomer in the solution, correlated linearly to the racemate concentration. It is noted from the slope of the linear regression that 94% of the desired enantiomer crystallized as DDS, while 80% of the undesired enantiomer was freely soluble in THF/H₂O (80/20) when 0.35 mol equiv of the resolving acid was used. Figure 9B shows that with the increase in racemate concentration, the slight gain in maximum yield was offset by the gradual loss in crystal *de*; however, the resolution efficiency was independent and optimally kept 0.60 at 40–140 mg/mL of racemate concentration. It is desirable for a scale-up resolution process to be conducted at a high racemate concentration, while achieving maximum resolution efficiency.

2.5. Solubility Phase Diagram of a Partial Solid Solution of Diastereomeric Salts. As part of development of a resolution process under thermodynamic equilibrium, an isothermal solubility phase diagram of diastereomeric salts at 25 °C (Figure 10) was constructed based on the optimal resolution

system identified (0.35 mol equiv of D-DATA, THF/H₂O, 80/20). A partial solid solution formed with a saturation point (B) of 14% UDS in DDS (72% *de*) as shown in Figure 10. For this partial solid solution forming salt reaction, the minimum molar equivalent of the resolving acid required for complete crystallization of DDS was calculated to be $0.25 \times (1 + 14/86/0.5) = 0.33$. This supports the optimal molar equivalent of 0.35 for D-DATA identified experimentally. The maximum resolution efficiency was determined to be 0.61 from the solubility phase diagram in Figure 10, consistent with the efficiency (0.60) calculated from the maximum yield and the crystal *de* under the same resolution conditions. Due to the formation of a partial solid solution, repetitive crystallization in THF/H₂O (80/20) was attempted but failed to effectively purify the isolated diastereomeric salt beyond 72% *de*.

Through characterization of the piperazine racemate, it was known that the racemic mixture with a minimum *ee* of 60% could be upgraded to a higher *ee* by crystallization in a proper solvent. Though a partial solid solution formed, the first step of classical resolution to obtain DDS/UDS mixture of *de* 72% was sufficient, and a second step of *ee* upgrade was then

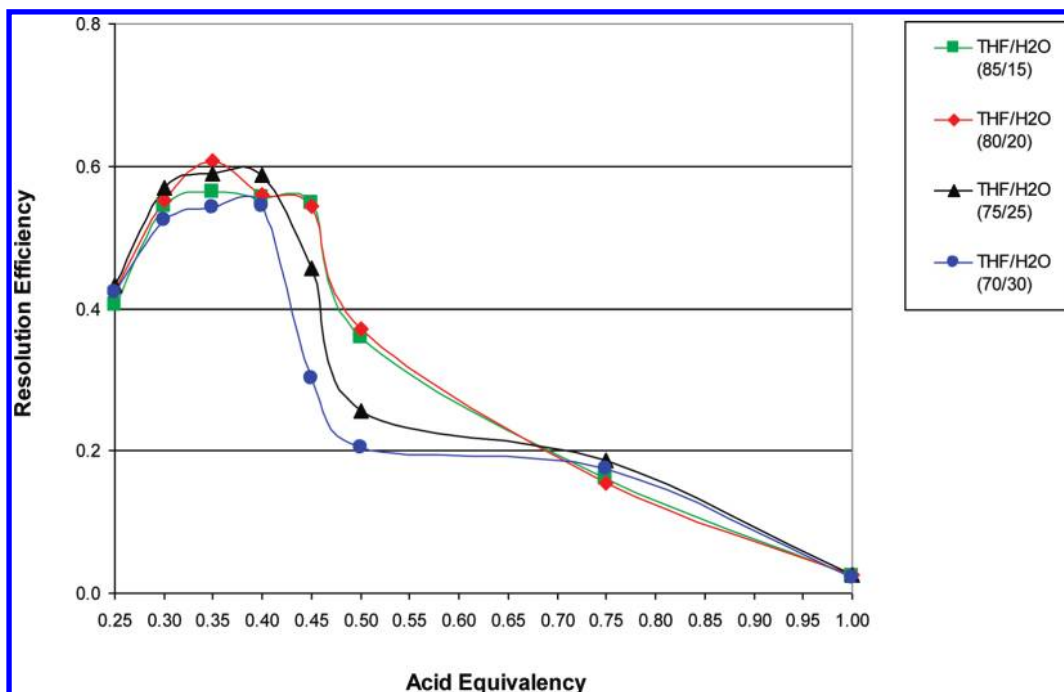


Figure 7. Resolution efficiency of DDS as related to the molar equivalent of *D*-DATA in THF/H₂O at a racemate concentration of 100 mg/mL.

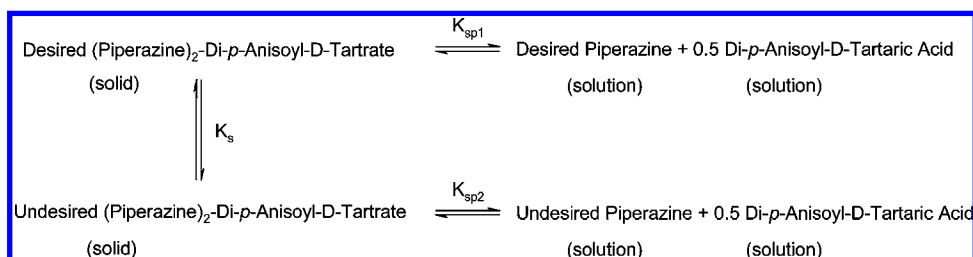


Figure 8. Solid-solution and solid-solid equilibria of DDS and UDS.

required. The freebase was highly soluble in most of organic solvents except *n*-heptane. The solubility of the racemate and the enantiopure isomer in *n*-heptane at 25 °C was 21.3 mg/mL and 6.4 mg/mL, respectively, and *n*-heptane was therefore chosen as the crystallization solvent for *ee* upgrade. The diastereomeric salt mixture was dissociated at the presence of NaOH, and the racemic piperazine mixture was extracted into MTBE then recrystallized in *n*-heptane to obtain the desired enantiomer $\geq 98\%$ *ee*.

2.6. Physicochemical Characterization of Diastereomeric Salts and Its Partial Solid Solution. DDS and UDS were synthesized by reacting the respective enantiopure piperazine with *D*-DATA in THF/H₂O (80/20). The solubility of DDS and UDS was 1.7 mg/mL and 16.5 mg/mL, respectively, in THF/H₂O (80/20) at 25 °C. To ensure that the thermodynamic-stable salt forms were obtained in the resolution solvent being used, DDS and UDS were slurried in THF/H₂O (80/20) through repetitive thermal cycles (50–5 °C) over three days. The XRPD patterns of two salts were distinctively different and remained unchanged through the thermal cycles. Moreover, a single polymorph of DDS or UDS was isolated from THF/H₂O (80/20) over a range of 0.25–1.0 mol equiv of *D*-DATA used, confirming the formation of the thermodynamic-stable DDS or UDS.

A quantitative HPLC assay was used to determine the ratio of *D*-DATA to the piperazine freebase in DDS and UDS. They were found to consist of two molecules of the freebase and one molecule of the acid. Solution ¹H NMR spectra were also acquired and analyzed to confirm that both were the hemisalts. TGA (Figure 11A, 11B) revealed both salts contained four molecules of water at equilibrium under ambient conditions. Continuous loss of water in DDS was observed upon heating from 25 to 90 °C, likely due to the presence of channel water. On the other hand, two stages of water loss occurred in UDS: the initial loss of two molecules of likely channel water from 25 to 50 °C, and subsequent loss of two molecules of possibly bonded water until 110 °C with an endotherm apex at 91.2 °C. After the water loss, the DSC melting point (Figure 11A, 11B) of DDS (130.0 °C) was lower than that of UDS (135.6 °C). Furthermore, it was found that desorption/absorption of water was reversible for DDS or UDS tetrahydrate after the salt was heated and re-equilibrated under ambient conditions. The solid-state data suggested that different properties (i.e., solubility, crystal form, hydration state) between DDS and UDS formed under thermodynamic equilibrium could mainly determine the efficiency of a resolving agent in a resolution solvent.

To further understand the characteristics of a solid solution, XRPD, DSC, and TGA were collected on an isolated sample

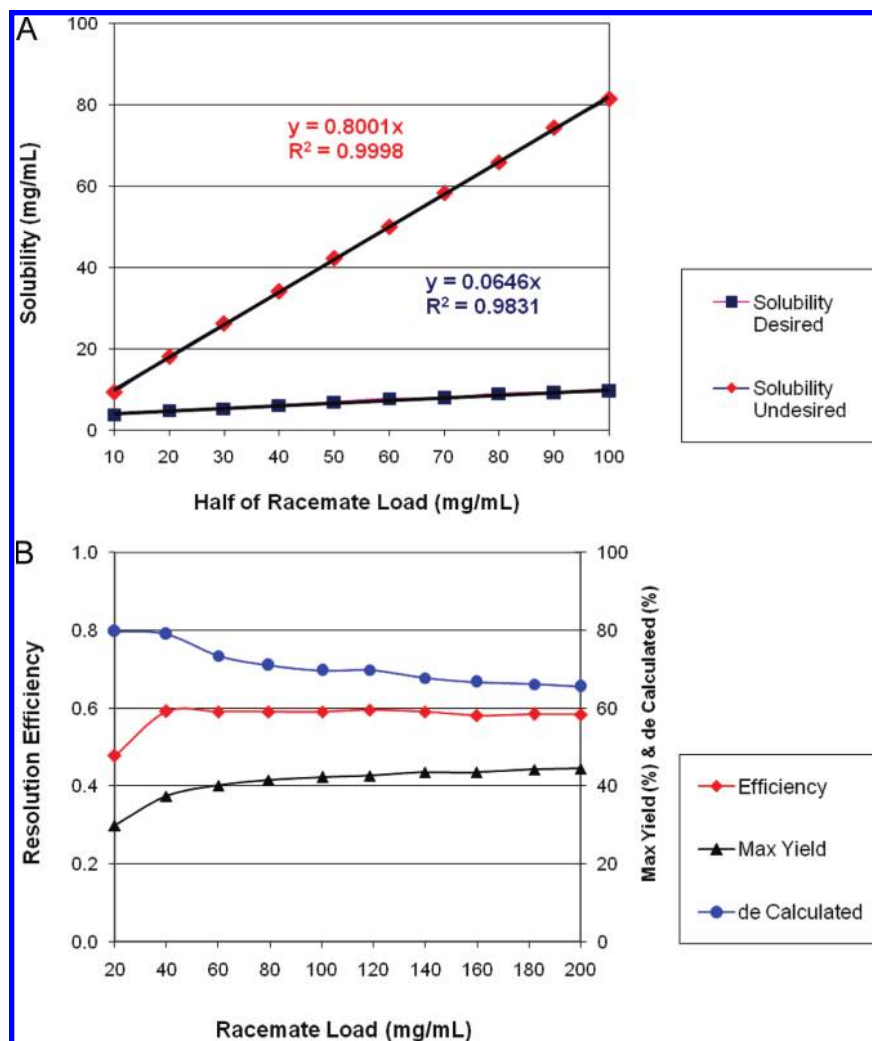


Figure 9. (A) Solubility of DDS and UDS formed with 0.35 mol equiv of *D*-DATA in THF/H₂O (80/20) as related to the racemate concentration. (B) Maximum yield, calculated *de*, and resolution efficiency of DDS formed with 0.35 mol equiv of *D*-DATA in THF/H₂O (80/20) as related to the racemate concentration.

of 72% *de*. Intuitively, the XRPD pattern of the solid solution sample was identical to that of DDS, revealing that up to 0.14 mole fraction of UDS could perfectly coexist in the crystal lattices of DDS. On the other hand, a solid blend (DDS:UDS = 86:14, mol %) was prepared and its XRPD pattern simply indicated a physical mixture of DDS and UDS. The DSC/TGA thermograms (Figure 11C) of the solid solution sample resembled those of DDS, indicating four molecules of likely channel water; however, the single melt of this solid solution at 131.0 °C was indistinctive between those of DDS (130.0 °C) and UDS (135.6 °C).

3. Conclusions

Representing a case study to resolve a racemic piperazine compound, a high throughput screening workflow in 96-well plate format has been developed and implemented for classical chiral resolution through diastereomeric salt crystallization. Based on the mass balance in each resolving system under screening, maximum yield, crystal *de*, and resolution efficiency were calculated from the solubility of diastereomeric salts measured under thermodynamic equilibrium. By screening 8 resolving acids in 12 solvent systems containing 0–50% water,

D-DATA and THF/H₂O (80/20) were identified to be the optimal resolution agent and solvent system to give the highest resolution efficiency. The effects of water as a cosolvent, resolving agent stoichiometry, and racemate concentration on the resolution efficiency were evaluated, and an isothermal solubility phase diagram was obtained for the optimal resolution system at 25 °C. Physicochemical characterization indicated that both DDS and UDS were hemitartrate tetrahydrates and they formed a partial solid solution with 72% *de*. The highest resolving efficiency (0.61) at 25 °C was observed with the optimal molar equivalent (0.35) of *D*-DATA, in agreement with the minimum molar equivalent (0.33) of *D*-DATA required for complete crystallization of DDS based on the solubility phase diagram. At a scale of 30 g of the piperazine racemate, the diastereomeric di-*p*-anisoyl-*D*-tartrate salt was crystallized in the optimal resolution system identified and collected at 0 °C with a resolution yield of 0.64 and 67% *de*. Given the fact that the racemic piperazine had a eutectic point of 60% *ee* characterized by its melting phase diagram, the obtained DDS/UDS solid solution was dissociated in NaOH solution and *ee* of the desired piperazine enantiomer was upgraded by recrystallization in *n*-heptane twice with an overall yield of 37% and 98% *ee*.

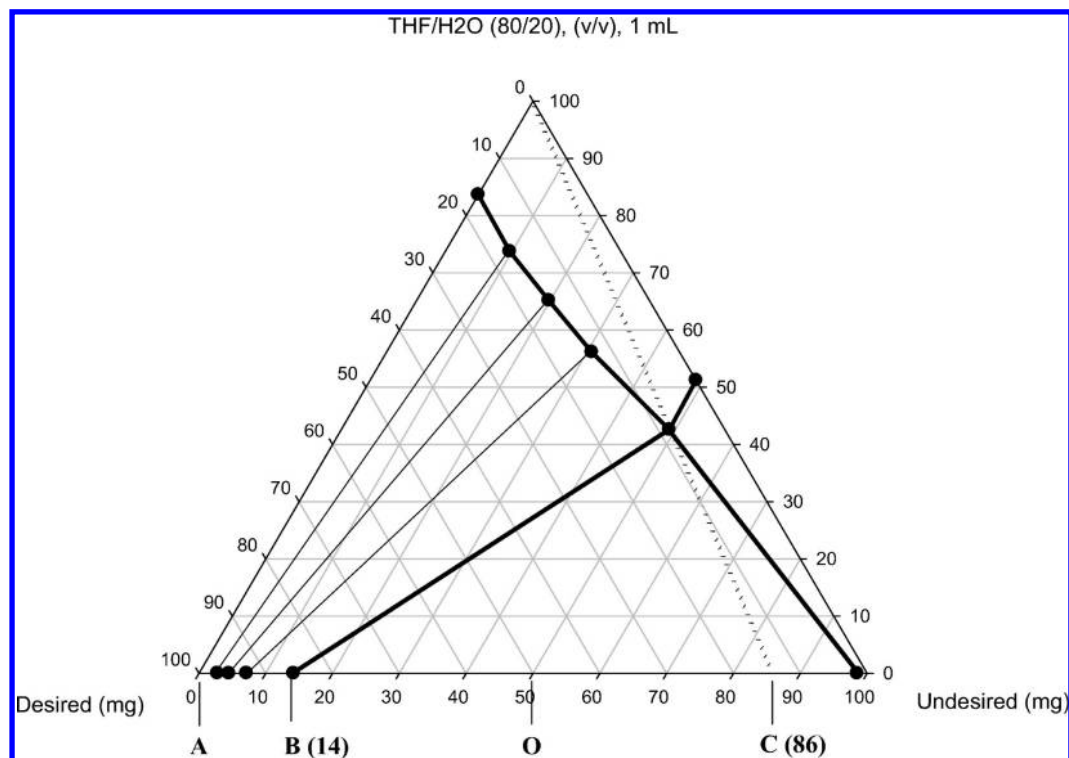


Figure 10. Solubility phase diagram of DDS and UDS in the optimal resolution system (0.35 mol equiv of D-DATA, THF/H₂O, 80/20). Maximum resolution efficiency = $2 \times [(OC - AB)/(AC - AB)] = 2 \times [(36 - 14)/(86 - 14)] = 0.61$.

Solubility is one of the most important factors in determining resolution efficiency of diastereomeric salt crystallization under thermodynamic equilibrium. Throughout this case study, the resolution efficiency in relation to the resolution conditions (resolving agent, solvent composition, resolving agent stoichiometry, and racemate concentration) was systematically evaluated by means of thermodynamic solubility measurements, mass balance calculations, and solubility phase diagram construction. In addition to solubility, solid-state properties (i.e., crystal form, hydrate state) are also determining factors in diastereomeric salt formation and crystallization. It is essential to characterize solid-state properties of the diastereomeric salts so as to understand their phase behaviors (i.e., formation of a partial solid solution) under thermodynamically favored resolution conditions. This case study demonstrated that the rational screening approach coupled with high-throughput experimentation is effective in rapidly guiding the scale-up of a classical resolution under thermodynamic equilibrium.

4. Experimental Section

Screening Procedures. The piperazine racemate was dispensed into 1-mL glass vials on a 96-well plate using a solid dispenser (*Symyx AutoDose*). The actual weight dispensed was recorded to the nearest 0.1 mg for mass balance calculation in each vial. Standard solutions of the resolving agents were prepared in MeOH, and calculated volumes of the resolving agent solutions were added at the appropriate molar ratio to the quantity of the racemate in each vial. The mixtures of the racemate and the resolving agent were dried using a vacuum centrifuge (*GeneVac HT 4*). A stir bar was added to each vial, and the vials were sealed with a 96-well cap mat. Following the solvent selection, 500 μ L of solvent were dispensed into

each vial using a liquid handler (*Symyx XCM*). The reaction mixtures were heated with stirring at 50 °C for 1 h and equilibrated at 25 °C for 24 h. The plate was then centrifuged, and a 96-well image viewing the bottoms of the vials was acquired using a polarized light microscope (*Zeiss Axiovert 2000*). Supernatant samples were taken from the vials, showing the white birefringence images and indicating crystallization of the diastereomeric salts, and the samples were diluted and analyzed by chiral HPLC for mother liquor *de* and solubility of the crystallized diastereomeric salts.

Construction of Solubility Phase Diagram of Diastereomeric Salts. Maintaining one enantiomer's amount at 30 mg while varying the others from 0 to 30 mg, racemic mixtures with different *ee* were prepared and subsequently mixed with 0.35 mol equiv of D-DATA in 0.5 mL THF/H₂O (80/20). The reaction mixtures were heated with stirring at 50 °C for 1 h and equilibrated at 25 °C for 24 h. The mother liquor sample was taken to determine the solubility of DDS and UDS crystallized. The crystallized salt was filtered, washed with THF/H₂O (80/20), and analyzed by chiral HPLC to obtain the relative mass percent of UDS to DDS. An isothermal solubility phase diagram at 25 °C (Figure 10) was constructed by plotting the solubility of DDS and UDS in 1 mL of THF/H₂O (80/20) and the relative mass percent of UDS to DDS in the crystallized solid for each resolution reaction (Point O: equimolar mixture of DDS and UDS; Point A: 100% DDS; Point B: partial solid solution of UDS (14%) saturated in DDS; Point C: the isoplethal projection of the saturated solution mixture of DDS and UDS towards the binary solid mixture of UDS (86%) and DDS).

Scale-Up of Diastereomeric Salt. A one L round bottle flask was charged with the piperazine racemate (0.1 mol) and 300 mL THF/H₂O (80/20). A solution of D-DATA was prepared

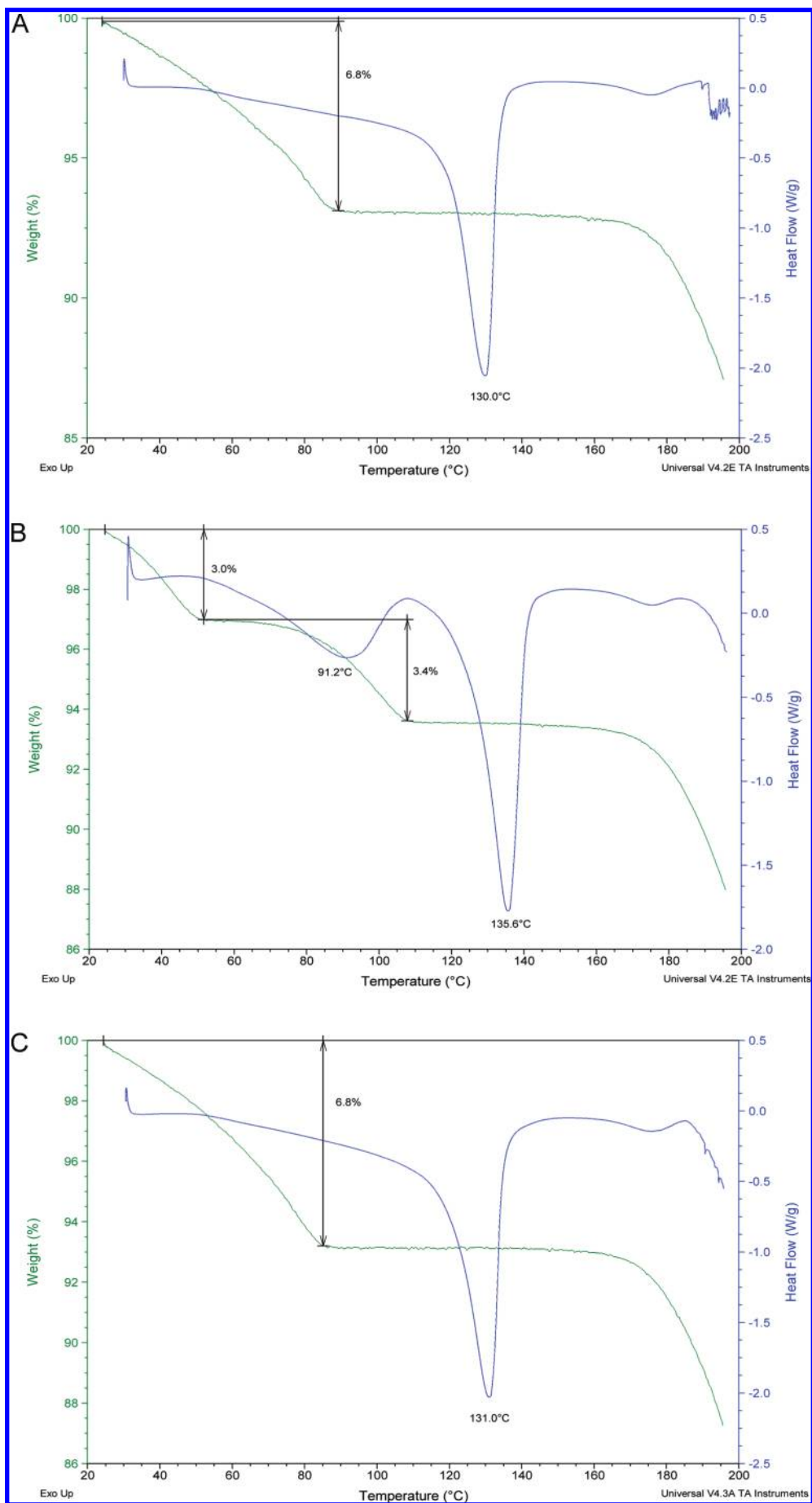


Figure 11. (A) DSC and TGA of DDS. (B) DSC and TGA of UDS. (C) DSC and TGA of a solid solution of DDS and UDS.

by mixing D-DATA (14.6 g, 0.035 mol) and 200 mL THF/H₂O (80/20). The flask was heated at 50 °C and a portion of D-DATA solution (40 mL) was added over 5 min. A seed of DDS (20 mg, 99% *de*) was then added and the reaction mixture was held at 50 °C for 20 min until a substantial seed bed was observed. The remaining D-DATA solution (160 mL) was slowly added over 4.5 h at 50 °C. Upon completing the addition, 100 mL THF/H₂O (80/20) was charged to the flask and the resulting slurry was stirred at 50 °C for 30 min and then slowly cooled down to 0 at 10 °C/h and held at 0 °C for 2 h. The slurry mixture was vacuum-filtered, the flask and the cake were rinsed with 2 × 80 mL 0 °C THF/H₂O (80/20). The solid was dried in the filter under N₂ stream for 16 h at 20 °C to give di-*p*-anisoyl-D-tartrate salt (29.1 g, 67% *de*; 6.8 wt % H₂O) as a white crystalline, with a yield of 48% corrected for *de* and water content. The resolution efficiency was 0.64 for DDS crystallized and recovered at 0 °C in this scale-up process.

ee Upgrade of Desired Enantiomeric Freebase. A 250 mL round-bottom flask was charged with 14.0 g di-*p*-anisoyl-D-tartrate salt (67% *de*, from the previous step) and 100 mL MTBE. A solution of 1 N NaOH (1 mol equiv) was added to the flask over 2 min. The mixture was stirred for 10 min until no solid was visible. The layers were then separated and the

organic layer was washed with 50 mL water and 50 mL brine sequentially. MTBE was distilled under the reduced pressure and 100 mL *n*-heptane was added to perform the solvent switch. After the solvent was distilled off, 22 mL *n*-heptane was added. The mixture was heated to 50 °C to afford a clear solution and then cooled down to 0 at 10 °C/h and held at 0 °C for 2 h. The crystallized solid was collected by vacuum filtration and dried in the filter under N₂ stream for 16 h at 20 °C to yield the free base (6.4 g, >99.5% achiral purity; 84.6% *ee*). The same recrystallization procedure was repeated in *n*-heptane to obtain the desired enantiomeric free base (5.6 g, 98.0% *ee*) as a white crystalline. The overall yield for entire resolution process (three steps) was 37%.

Acknowledgment

We thank Jerry Murry for suggestion and support of high-throughput chiral resolution screening assay development and implementation, and Janan Jona for advice and review of this manuscript.

Received for review September 1, 2010.

OP1002402